# THERMOECONOMIC SIMULATION OF A COMPLEX ENERGY SYSTEM FOR PERFORMANCE ANALYSIS AND PREDICTION IN DEEP PEAK SHAVING

***Sha LIU[1*], Jiong SHEN[2], Junli ZHANG[2], Xiao WU[2]***

[*1]School of Mechanical and Electrical Engineering, Jinling Institute of Technology, Nanjing 211169, China

[2]National Engineering Research Center of Power Generation Control and Safety, School of Energy and Environment, Southeast University, Nanjing 210096, China, School of Energy and Environment, Southeast University, Nanjing, 210096, China

[*]Corresponding author: Sha Liu; E-mail: liusha@jit.edu.cn

*The establishment of a cost model for complex energy systems based on thermoeconomics can provide technical and economic evaluation indicators for complex energy systems. At the same time, to integrate more renewable energy into the grid, complex energy systems must participate in deep peak shaving. To evaluate the technical-economic performance of complex energy systems involved in deep peak shaving, a novel thermoeconomic cost construction method is proposed based on the production structure diagram, using the gas-steam combined cycle system as an example. these can effectively avoid the derivation error of high-dimensional models, improve the modeling and calculation speed, and obtain the variation trend of system thermoeconomics cost under load changes and operating parameter changes. The results show that the external and internal factor can change the power generator thermoeconomic cost. the power generation cost of the system increases with increasing natural gas price and environmental temperature When the compressor pressure ratio increases, the power generation cost of the system also increases. At 100% load, the power generation cost reaches its lowest value when the exhaust temperature is equal to 615 ℃.*

Key words: *complex energy systems; deep peak shaving; performance analysis; performance prediction; thermoeconomic cost*

## 1. Introduction

Through the performance analysis of complex energy systems, we can determine the mechanism of performance degradation and improve the system performance. With the development of modern thermodynamic analysis methods, various methods for analyzing and evaluating complex energy systems have emerged: 1) the energy analysis method, 2) the exergy analysis method, and 3) the thermoeconomic analysis method [1,2].

Complex energy systems are not only technically superior but also economically reasonable. The thermoeconomic analysis method is used to analyze and optimize both technical and economic factors, providing the basis for technical and economic decision-making. The basic concept of the thermoeconomic analysis method is to regard the interacting substances, energy, exergy, and cash in the thermodynamic system as "flows," which flow in or out from a certain part of the system [3-4]. In the process of flow, the relevant trends of the physical environment and economic environment are observed, and these trends can be described by a series of mathematical equations. These mathematical equations usually include the mass balance equation, energy balance equation, exergy balance equation, and cost balance equation. In thermoeconomics, the key link is the establishment of a cost balance equation [5-9].

The thermoeconomic structure theory is the most important model in the thermoeconomic analysis method. The thermoeconomic structure theory divides the system into several production components [10-14]. The cost balance equation is constructed based on the production structure diagram. In the research on the thermoeconomic cost modeling, the existing unit cost equation modeling method is the chain differential law. Reference [15] applied the chain differential law to analyze the total cost of gas turbine combined cycle (GTCC) power plant. Reference [16] established an environmental thermoeconomic cost model of GTCC based on the chain differential law of thermoeconomics. And then an annual total cost model is established, which can reflect the real economic performance. Reference [17] studied thermoeconomic cost for GTCC under different operating strategies based on the chain differential law.

However, several problems exist with the use of the chain differential law. Due to the increase in the number of system production components and the increase in the virtual components, when complex energy systems are analyzed and the chain differential rule is used to establish the unit cost equation, the modeling speed is slow, and the process of deriving the partial differential equation is complex [18-20]. Moreover, when a complex energy system participates in deep peak shaving, a more rapid calculation method needs to be developed for the online calculation of the thermoeconomic cost of the system under multiple conditions.

To address the above problems, a novel method is proposed to establish a unit thermoeconomic cost equation for complex energy systems. The establishment criteria of the unit thermoeconomic cost equation for different types of components are given by combining the input and output relationships of each component in the production structure diagram. This method has a high modeling speed and avoids derivation errors when using the chain differential method. Using the gas-steam combined cycle system as an example and considering regional differences, the influence of the natural gas price changes on the thermoeconomic cost of the combined cycle system is examined. Considering seasonal differences, the impact of environmental temperature changes on the thermoeconomic cost of the combined cycle system is studied. Based on the importance of the internal parameters of the system, the impact of the compressor pressure ratio and exhaust temperature changes on the thermoeconomic cost of the combined cycle system are also investigated. Simulation calculations show that this method can effectively meet the computational requirements for the response trends of the thermoeconomic indicators when the operating conditions of complex energy systems change, providing a foundation for the evaluation and operation optimization of complex energy systems.

This manuscript is organized as follows. A thermoeconomic cost performance analysis and prediction modeling method is proposed in the second section. In the third section, the methodology is validated through an example analysis, and the results with different disturbance factors are discussed. In Section IV, the main conclusions obtained in this study are provided.

## 2. Thermoeconomic cost performance analysis and prediction modeling

In the modeling process of complex energy systems, first, the components are divided, and a thermodynamic model is established that includes the mass conservation equation, energy conservation equation, energy balance equation, and cash balance equation. A diagram of the physical structure of complex energy systems is created, and a diagram of the production structure is developed based on the definitions of fuel and products. A thermoeconomics structure cost equation is constructed, and a thermoeconomics cost model of a complex energy system is established.

The exergyeconomics cost model of the complex energy system is shown in Fig. 1.

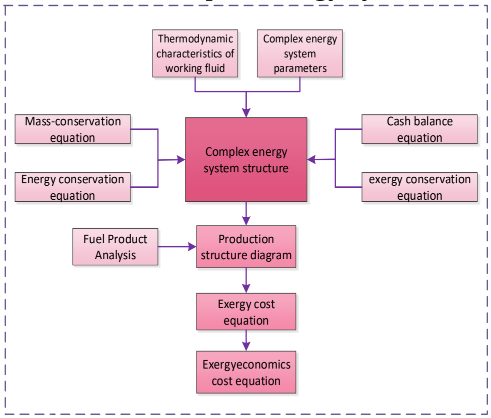


**Fig. 1. Thermoeconomic model of a complex energy system**

### 2.1. Fuel products of complex energy systems

The object of thermoeconomics structural theory analysis is complex energy systems, including multiple production process units, which are interconnected through exergy flow. The purpose of an energy system is to output one or more terminal energy flows as products, where the production process units complete the intermediate energy conversion process and output intermediate products. To obtain a certain intermediate product energy flow or terminal product energy flow, the external energy input to the system is needed, and the other production resources are consumed. In the energy system, the cost of forming an energy flow represents all external resources that must be provided to the entire energy system to produce this energy flow.

The monetary cost of energy flow refers to the amount of money required to produce that energy flow, including the cash flow equivalent to the input fuel, as well as equipment procurement, installation, operation, maintenance, and repair (OM&R) expenses. The unit monetary cost of the energy flow is also known as the unit thermodynamic cost and is the amount of money required to produce a unit of energy flow.

The function of the production process unit in the energy system is to produce a certain amount of energy product. Therefore, from the perspective of production, the output exergy flow is called the product, with the symbol P. To obtain the products, the production process unit must consume a certain amount of energy, and these input exergy flows are also represented by the exergy flow, called fuel, symbol F. The actual thermal process is irreversible; thus, the product of the production process unit is always smaller than the fuel, and its fire balance equation is as follows:

$$F = P + I \tag{1}$$

where $F$ is the fuel exergy, kW; $P$ represents the product exergy, kW; and $I$ refers to the irreversible loss (exhaust loss), kW.

Therefore, fuel exergy consumption is also related to the irreversible loss of the process and can be characterized by unit exergy consumption kB, as shown in Eq. (12):

$$k = \frac{F}{P} \tag{2}$$

where $kB$ is the unit exergy consumption, kW/kW.

### 2.2. Productive structure diagram

The production structure diagram of a complex energy system is based on a physical model that describes the production relationship between the process units; specifically, these units include the distribution of fuel, products, and resources of all process units in the system. The component corresponding to the actual equipment in the physical model is also a component in the production structure diagram; however, the relationship between the energy flow is different from that in the physical model. At the same time, virtual process units are used to represent energy flow relationships in the production structure diagram. The components in the production structure diagram have the following characteristics:

(1) In the production structure diagram, the exergy flows of all production components corresponding to the actual equipment are single inputs and outputs.

(2) In the production structure diagram, the two types of virtual components are the junction components and branch units. A junction is represented by a prism and refers to the fusion of products from two or more production components at the junction point; this forms the fuel of another production component. The branches are represented by circles and refer to the exergy flow that is divided into two or more streams in a branch unit and subsequently becomes fuel for two or more downstream process units.

(3) The investment in the components corresponding to the actual equipment, as well as the monetary costs of operation, maintenance, and repair (OM&R), are used as external resources to enter this process unit.

### 2.3. Thermoeconomic structure diagram

The thermoeconomic model of complex energy systems is a mathematical model that describes the energy production relationship in a production structure diagram.

The production components i formed by actual equipment have an input fuel of $F_i$ and an output product of $P_i$. The thermoeconomic model of these production components provides a mathematical relationship between fuel and product, as follows:

$$F_i = g_i(x_i, P_i) \tag{3}$$

where $x_i$is the internal performance parameter of the component.

For virtual components, a cost allocation plan for energy flow convergence and branching needs to be provided. The input and output characteristics of the actual equipment are processed using linear relationships. In the structural theory of thermoeconomics, the following linear characteristic equations are used:

(1) For the production component, its unit exergy consumption coefficient $k_i$ is used as the performance parameter:

$$F_i = k_i P_i \tag{4}$$

(2) For the junction component Ji, assuming there are m input exergy flows $B_1$, $B_2$, …, $B_m$ and one output exergy flow $B_{ji} = \sum_{i=1}^{m} B_i$, the performance parameter is the relative share of each input flow:

$$r_1 = \frac{B_1}{B_{Ji}}, r_2 = \frac{B_2}{B_{Ji}}, \cdots, r_m = \frac{B_m}{B_{Ji}}, \sum_{i=1}^{m} r_i = 1 \tag{5}$$

(3) For branch components, the input exergy flow is equal to the sum of the output exergy flows, and the cost of each output exergy flow is equal to the cost of the input exergy flow.

When comprehensively examining the thermoeconomic cost of a product, all production process components corresponding to actual equipment need to be injected with monetary costs. The monetary cost equation of the equipment refers to the relationship among the investment, operation, maintenance, repair (OM&R) costs, thermodynamic parameters, and equipment products. In thermoeconomic structural theory, a system is entered in a fixed-cost manner. Both exergy and currency can be regarded as general equivalents, and the cost of energy flow can be expressed in currency. The mathematical expression for the unit thermoeconomic cost equation considering nonenergy costs is as follows:

$$C_{Pi}^* = k_i C_{Fi}^* + Z_i^* \tag{6}$$

## 3. Case study and results analysis

### 3.1. Establishment of the production structure diagram

The performance prediction model is verified using the test data of a 255 MW gas-steam combined cycle unit (GSCC). The thermodynamic system diagram of the unit is shown in Fig. 2. The thermodynamic system diagram of the unit is shown in Fig. 3.

The gas turbine model is PG9351FA, the compressor pressure ratio is 15.4, and the low heat generation of natural gas is 48686.3 kJ/kg. Under 100% load design conditions, the fuel mass flow rate is 50.1 t/h, the atmospheric pressure is 101.1 kPa, the temperature is 17.4 ℃, and the relative humidity is 78.89%.

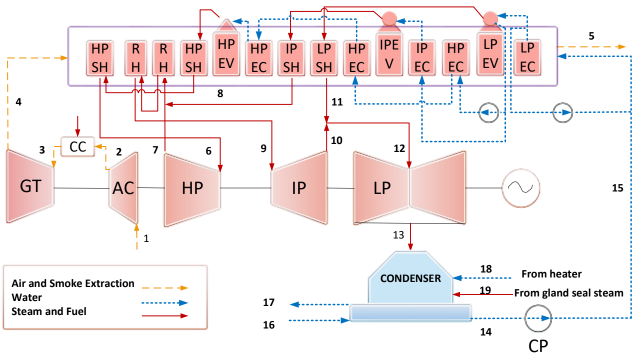


**Fig. 2. Thermodynamic system diagram of the GSCC**

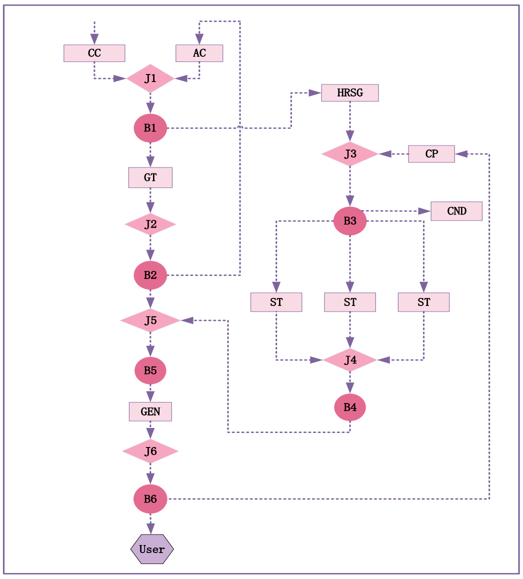


**Fig. 3. Production structure diagram**

### 3.2. Establishment of the unit thermoeconomic cost

The unit thermoeconomic cost equation for each component (listed in Tab. 1) is established based on the combined cycle production structure diagram. In the process of constructing the unit thermoeconomic cost of a component, external resources such as natural gas, coal, and oil are input into the component, and the unit fuel thermoeconomic cost is equal to the price of the resources (such as natural gas, coal, or oil). The same branch component outputs the same unit fuel thermal economic cost. The unit product thermoeconomic cost of the branching components is equal to the sum of the weights of the unit fuel thermoeconomic costs.

**Tab. 1. Establishment of the unit thermoeconomic cost equation**

| Number | Component | Unit fuel thermoeconomic cost | Unit product thermoeconomic cost |
|---|---|---|---|
| 1 | AC | $C_{F1}^* = C_{P3}^*$ | $C_{P1}^* = k_1 C_{F1}^* + Z_1^*$ |
| 2 | CC | $C_{F2}^* = \text{price}_{NG}$ | $C_{P2}^* = k_2 C_{F2}^* + Z_2^*$ |
| 3 | GT | $C_{F3}^* = r_1 C_{P1}^* + r_2 C_{P2}^*$ | $C_{P3}^* = k_3 C_{F3}^* + Z_3^*$ |
| 4 | HRSG | $C_{F4}^* = r_1 C_{P1}^* + r_2 C_{P2}^*$ | $C_{P4}^* = k_4 C_{F4}^* + Z_4^*$ |
| 5 | HP | $C_{F5}^* = r_4 C_{P4}^* + r_9 C_{P9}^*$ | $C_{P5}^* = k_5 C_{F5}^* + Z_5^*$ |
| 6 | IP | $C_{F6}^* = r_4 C_{P4}^* + r_9 C_{P9}^*$ | $C_{P6}^* = k_6 C_{F6}^* + Z_6^*$ |
| 7 | LP | $C_{F7}^* = r_4 C_{P4}^* + r_9 C_{P9}^*$ | $C_{P7}^* = k_7 C_{F7}^* + Z_7^*$ |
| 8 | CND | $C_{F8}^* = r_4 C_{P4}^* + r_9 C_{P9}^*$ | $C_{P8}^* = k_8 C_{F8}^* + Z_8^*$ |
| 9 | CP | $C_{F9}^* = C_{P10}^*$ | $C_{P9}^* = k_9 C_{F9}^* + Z_9^*$ |
| 10 | GEN | $C_{F10}^* = r_{5,6,7}(\sum_{i=5}^{7} r_i C_{Pi}^*) + r_3 C_{P3}^*$ | $C_{P10}^* = k_{10} C_{F10}^* + Z_{10}^*$ |

### 3.3. Simulation of the performance prediction model under parameter disturbance

To verify the combined cycle thermoeconomics model, using the combined cycle thermal system in Fig. 2 as an example, three typical loads of 50%, 75%, and 100% were selected to calculate the power generation cost (thermoeconomics cost of the system). The main parameters of each flow (The energy flow numbers correspond to Fig. 2) under 50% and 75% 100% loads are listed in Tab. 2. The parameters in Tab. 2 are used to calculate the exergy value of each energy flow.

**Tab. 2. Establishment of the unit thermoeconomic cost equation**

| Number | Quality | | | Pressure | | | Temperature | | | Specific enthalpy | | |
|---|---|---|---|---|---|---|---|---|---|---|---|---|
| | $M_i$(t/h) | | | $P_i$(kPa) | | | $T_i$(℃) | | | $H_i$(kJ/kg) | | |
| | 50% | 75% | 100% | 50% | 75% | 100% | 50% | 75% | 100% | 50% | 75% | 100% |
| 1 | 1396.8 | 1760.5 | 2270.2 | 101.1 | 101.1 | 101.1 | 17.4 | 17.4 | 17.4 | 42.3 | 42.3 | 42.3 |
| 2 | 1396.8 | 1760.5 | 2270.2 | 1556.9 | 1556.9 | 1556.9 | 422.2 | 422.2 | 422.2 | 456.9 | 456.9 | 456.9 |
| 3 | 1425.8 | 1800 | 2329.9 | 1533.6 | 1533.6 | 1533.6 | 1232.1 | 1291.3 | 1273.2 | 1444.9 | 1516.1 | 1494.3 |
| 4 | 1425.8 | 1800 | 2329.9 | 102.4 | 103.1 | 104.4 | 648.9 | 643.6 | 607.1 | 744 | 737.6 | 693.8 |
| 5 | 1425.8 | 1800 | 2320.3 | 101.1 | 101.1 | 101.1 | 74.9 | 76.8 | 83.8 | 54.1 | 56.4 | 64.8 |
| 6 | 198.5 | 240.1 | 280.9 | 6812 | 8210 | 9563 | 565.7 | 565.6 | 565.5 | 3568.6 | 3555.3 | 3542.2 |
| 7 | 190.3 | 230.2 | 280.9 | 1675 | 2066 | 2410 | 367.8 | 369.2 | 367.9 | 3184 | 3179.9 | 3170.6 |
| 8 | 23.5 | 29.6 | 38.8 | 1650 | 2038 | 2386 | 280 | 291.4 | 300.4 | 2988.9 | 3003.6 | 3014.7 |
| 9 | 214.3 | 265.2 | 309.5 | 1486 | 1841 | 2146 | 561.4 | 565.5 | 565.5 | 3607.6 | 3613.5 | 3610.7 |
| 10 | 213.3 | 264.2 | 309.5 | 242.2 | 306 | 365.4 | 305.9 | 310.9 | 313.5 | 3083.1 | 3091.7 | 3095.6 |
| 11 | 19 | 28.8 | 41.4 | 316.6 | 331.4 | 408.6 | 276.1 | 286.4 | 295.2 | 3020.5 | 3041 | 3057.1 |
| 12 | 232.3 | 293 | 361 | 242.2 | 306 | 365.4 | 305.9 | 310.9 | 313.5 | 3083.1 | 3091.7 | 3095.6 |
| 13 | 232.3 | 293 | 361 | 4.721 | 5.281 | 5.857 | 31.9 | 33.9 | 35.7 | 2447.6 | 2428.9 | 2418.6 |
| 14 | 262 | 330.5 | 395 | 4.721 | 5.281 | 5.856 | 31.9 | 33.9 | 35.7 | 133.5 | 141.8 | 149.7 |
| 15 | 262 | 330.5 | 395 | 2544 | 2506 | 2460 | 32.4 | 34.3 | 36.1 | 138.2 | 145.8 | 153.2 |
| 16 | 23742.1 | 23742.1 | 23742.1 | 344.7 | 344.7 | 344.7 | 23.7 | 23.7 | 23.7 | 99.7 | 99.7 | 99.7 |
| 17 | 23742.1 | 23742.1 | 23742.1 | 275.8 | 275.8 | 275.7 | 29.4 | 30.7 | 32 | 123.2 | 129 | 134.4 |
| 18 | 20.3 | 26.5 | 32.5 | 4846 | 4706 | 4593 | 54.2 | 55.8 | 58.1 | 231.1 | 237.5 | 247.1 |
| 19 | 1.2 | 1.2 | 1.4 | 100 | 100 | 100 | 99.6 | 99.6 | 99.6 | 1652.3 | 1685.6 | 1919.5 |

#### *3.3.1 Natural gas price disturbance*

Considering regional differences, the impact of natural gas price changes on the power generation cost of a combined cycle system under three typical loads (50%, 75%, and 100%) was examined, with natural gas prices ranging from 0.5 to 2.5 yuan/m$^3$, a low heat generation of 48686.3 kJ/kg, a flow rate of 50.1 t/h, an atmospheric pressure of 101.1 kPa, a temperature of 17.4 ℃, and a relative humidity of 78.89%. The reference point for calculating exergy in this manuscript is 101.1kPa (Atmospheric pressure) and 17.4 ℃ (Reference temperature)

Fig. 4 shows the power generation cost with natural gas price disturbances under different output power loads.

When the price of natural gas is constant, a higher load of the unit correlates to a lower power generation cost (thermoeconomic cost of the unit) of the combined cycle system. When the unit is under arbitrary load, and the equipment investment cost of the unit remains the same, but the higher the load, the higher the exergy efficiency of the unit, the lower the exergy consumption of the unit, and the lower the thermoeconomic cost of the unit. When the load is constant, the power generation cost of the combined cycle system increases with increasing natural gas price. When the natural gas price changes from 0.5 yuan/m$^3$ to 2.5 yuan/m$^3$ at 100% load, the power generation cost of the combined cycle system increases from 0.1577 yuan/(kW·h) to 0.5272 yuan/(kW·h).

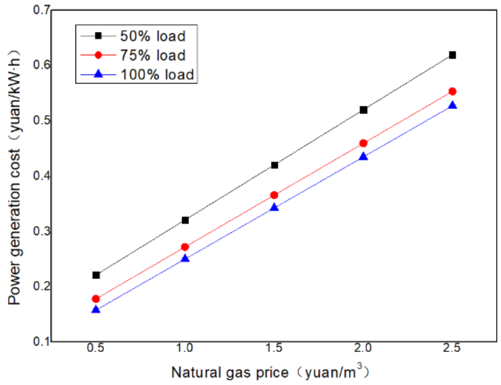


**Fig. 4. Power generation cost with natural gas price disturbances under different output power loads**

### *3.3.2 Ambient temperature disturbance*

Considering the seasonal differences, the impact of environmental temperature changes on the power generation cost of a combined cycle system under three typical loads (50%, 75%, and 100%) was examined, with an ambient temperature of 5-30 ℃, a natural gas price of 1 yuan/m$^3$, a low heat generation of 48686.3 kJ/kg, a flow rate of 50.1 t/h, an atmospheric pressure of 101.1 kPa, and a relative humidity of 78.89%.

Fig. 5 shows the power generation cost with the ambient temperature disturbance under different output power loads.

When the unit load is constant, the power generation cost of the combined cycle system increases with increasing environmental temperature; these results indicate that the power generation cost of the gas-steam combined cycle system decreases in winter and increases in summer. On the other hand, when the ambient temperature is less than 15 ℃, the impact of unit environmental temperature changes on the power generation cost is relatively small; when the ambient temperature exceeds 15 ℃, the change in unit ambient temperature has a significant impact on the power generation cost. Additionally, as the unit load increases, the impact of the unit environmental temperature changes on the power generation cost of the combined cycle system decreases.

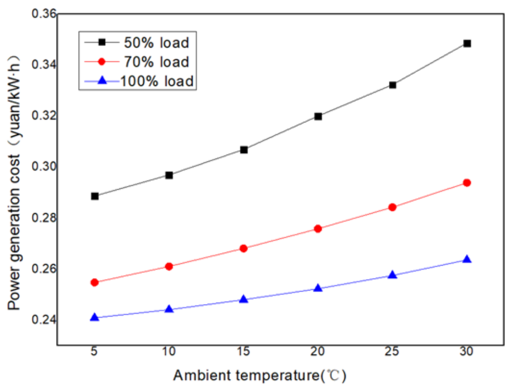


**Fig. 5. Power generation cost with ambient temperature disturbance under different output power loads**

### *3.3.3 Compressor pressure ratio disturbance*

The environmental temperature is 17.4 °C, the natural gas price is 1 yuan/m$^3$, the low heat generation is 48686.3 kJ/kg, the flow rate is 50.1 t/h, the atmospheric pressure is 101.1 kPa, and the relative humidity is 78.89%. The impact of the changes in the compressor pressure ratio on the power generation cost of the combined cycle system under three typical loads (50%, 75%, and 100%) is examined.

Fig. 6 shows the power generation cost with respect to the compressor pressure ratio disturbance under different output power loads.

Usually, increasing the pressure ratio of the compressor will increase the power consumption of the compressor, and also increase the external work of the gas turbine. In order to obtain the maximum net work, there must be an optimal pressure ratio; Increasing the pressure ratio of the compressor will improve the thermal efficiency of the combined cycle. This manuscript aims to minimize the power generation cost of the system and analyzed the impact of compressor pressure ratio on the power generation cost of the system. When the compressor pressure ratio is constant, a larger load of the unit correlates to a lower power generation cost. When the compressor pressure ratio increases, the power generation cost of the system decrease. Therefore, when materials and economic conditions permit, the maximum pressure ratio should be selected during the design.

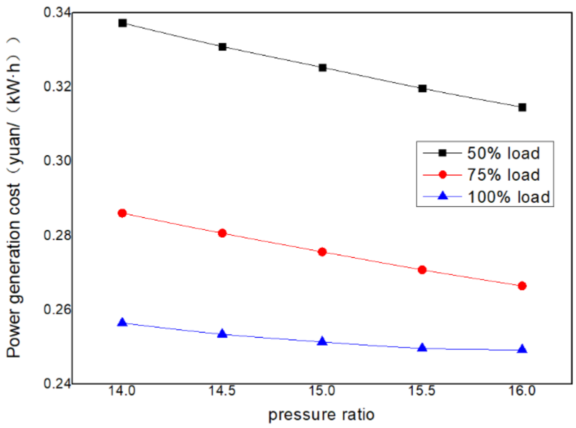


**Fig. 6. Power generation cost with the compressor pressure ratio disturbance under different output power loads**

### *3.3.4 Exhaust temperature disturbance*

Fig. 7 shows the power generation cost with respect to the exhaust temperature disturbance under the different output power loads.

As the exhaust temperature of the gas turbine increases, the power generation cost of the combined cycle system initially decreases and then increases. At 100% load, the power generation cost reaches its lowest value when the exhaust temperature is equal to 615 °C. This occurs mainly because when the exhaust temperature is high (above 615 °C), the irreversible heat transfer loss caused by the temperature difference in the waste heat boiler is greater, and the exhaust temperature of the waste heat boiler increases, causing more losses. When the exhaust temperature is low (below 615 °C), the irreversible loss of the combustion chamber increases, and the power output of the entire combined cycle system decreases.

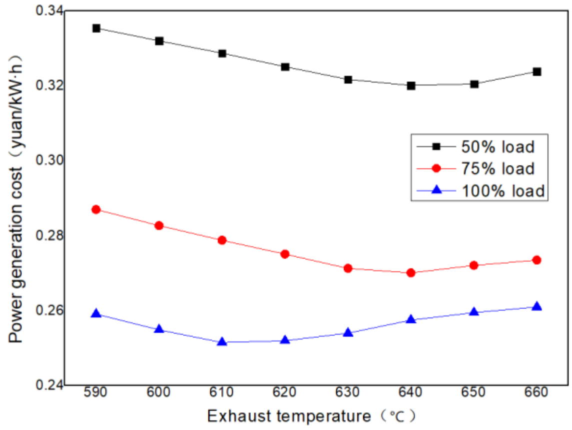


**Fig. 7. Power generation cost with exhaust temperature disturbance under different output power loads**

## 4. Conclusions

For a unit participating in deep peak shaving, a performance analysis and prediction model for complex energy systems based on thermoeconomics is established. The following conclusions can be drawn:

(1) The impact of the external factor changes is analyzed. When the load is constant, the power generation cost of the combined cycle system increases with increasing natural gas price and environmental temperature

(2) The impact of internal parameter changes is analyzed, When the compressor pressure ratio increases, the power generation cost of the system decrease. As the exhaust temperature of the gas turbine increases, the power generation cost of the combined cycle system initially decreases and then increases. At 100% load, the power generation cost reaches its lowest value when the exhaust temperature is equal to 615 ℃.

Considering the carbon neutrality policy of the Chinese government, the environmental impact should be included in the thermoeconomic structural theory analysis and optimization in future studies. In the process of the thermoeconomic structure theory analysis of the combined cycle system, this paper only considers the impact of energy costs and non-energy costs on the system, and carbon emission cost should be added to the establishment of thermoeconomic costs model in the future.

## Acknowledgments

This work was supported by the National Natural Science Foundation of China (NSFC) under Grant 52206013 and the National Natural Science Foundation of China (NSFC) under Grant 51936003.

## Nomenclature

| **Acronyms** | | **Symbols** | |
|---|---|---|---|
| AC | air compressor | F | fuel exergy, [kW] |
| CC | combustion chamber | P | product exergy, [kW] |
| CP | condensate pump | I | irreversible loss, [kW] |

| | | | |
|---|---|---|---|
| CND | condenser | $c_P^*$ | unit output exergy economic cost of equipment, [yuan/(kW·h)] |
| GT | gas turbine | $c_F^*$ | unit input exergy economic cost of equipment, [yuan/(kW·h)] |
| GNE | generator | $k$ | unit exergy consumption of equipment kW/kW |
| HP | high pressure cylinder | $Z^*$ | unit nonenergy cost of equipment, [yuan/(kW·h)] |
| IP | intermediate pressure cylinder | $r_i$ | exergy flow rate |
| LP | low pressure cylinder | $price_{fuel}$ | external fuel prices, [yuan/(kW·h)] |
| HRSG | waste heat boiler | $P_i$ | pressure of each energy flow, [kPa] |
| J | collection components | $T_i$ | temperature of each energy flow, [°C] |
| B | branch components | $H_i$ | specific enthalpy of each energy flow, [kJ/kg] |

**References**


[1] Köse, Ö., *et al*., Performance Improvement of the Bottoming Steam Rankine Cycle (SRC) and Organic Rankine Cycle (ORC) Systems for a Triple Combined System Using Gas Turbine (GT) as Topping Cycle, *Energy Convers. Manag*., *211* (2020), pp. 112745

[2] Wang, S. K., *et al*., Techno-Economic-Environmental Evaluation of a Combined Cooling Heating and Power System for Gas Turbine Waste Heat Recovery, *Energy*, *231* (2021), pp. 1246

[3] Ren, J., *et al*., Thermodynamic, Exergoeconomic, And Exergoenvironmental Analysis of a Combined Cooling and Power System for Natural Gas-Biomass Dual Fuel Gas Turbine Waste Heat Recovery, *Energy*, *269* (2023) , pp. 126676

[4] Kler, A. M., *et al*., Co-Optimization of Thermal Power Plant Flowchart, Thermodynamic Cycle Parameters, and Design Parameters of Components, *Energy*, *193* (2020), pp. 116679

[5] von Spakovsky, M. R., Application of Engineering Functional Analysis to the Analysis and Optimization of the CGAM Problem, *Energy*, *19* (1994), 3, pp. 343-364

[6] Bejan, A. *Advanced engineering thermodynamics*, Wiley., New York, USA, 1988.

[7] Jamil, M. A., A Comprehensive Framework for Thermoeconomic Analysis of Desalination Systems, *Energy Convers. Manag*., *222* (2020), pp. 113188

[8] Pan, J., *et al*., Energy, Exergy and Economic Analysis of Different Integrated Systems for Power Generation Using LNG Cold Energy and Geothermal Energy, *Renewable Energy*, *202* (2023), pp. 1054-1070

[9] Lucia, U., *et al*., A Thermoeconomic Indicator for the Sustainable Development with Social Considerations, *Environment, Development and Sustainability*, 24 (2021), pp. 2022-2036

[10] Takleh, H., *et al*., Proposal and Thermoeconomic Evaluation with Reliability Considerations of Geothermal Driven Trigeneration Systems with Independent Operations for Summer and Winter, *International Journal of Refrigeration*, *127* (2021), pp. 34-46

[11] Valero, A., *et al*., On the Thermoeconomic Approach to the Diagnosis of Energy System Malfunctions: Part 1: the TADEUS Problem, *Energy*, *29* (2004), pp. 1875-1887

[12] Valero, A., *et al*., On the Thermoeconomic Approach to the Diagnosis of Energy System Malfunctions: Part 2: Malfunctiondefinitions and Assessment, *Energy*, *29* (2004), pp. 1889-1907

[13] Torres, C., Antonio, V., The Exergy Cost Theory Revisited, *Energies*, *146* (2021), pp. 1-43

[14] Chu, S. L., *et al*., Energy, Exergy, Energy-Saving, Economic and Environmental Analysis of a Micro-Gas Turbine-PV/T Combined Cooling, Heating and Power (CCHP) System under Different Operation Strategies: Transient Simulation, *Energy Conversion and Management*, *276* (2023), pp. 116557

[15] Wu, Z., *et al*., An Efficient Methanol Pre-Reforming Gas Turbine Combined Cycle with Integration of Mid-Temperature Energy Upgradation and $CO_2$ Recovery: Thermodynamic and Economic Analysis, *Applied Energy*, *358* (2024), pp. 122599

[16] Wang, Z., *et al*., Multi-Objective Optimization of Gas Turbine Combined Cycle System Considering Environmental Damage Cost of Pollution Emissions, *Energy*, *261* (2022), pp. 125279

[17] Wang, Z., *et al*., Thermoeconomic Cost Analysis on Operation Strategies of Gas Turbine Combined Cycle under Off-Design Conditions, *Case Stud. Therm. Eng*., *28* (2021), pp.101617

[18] Valero, A., César, T., Relative Free Energy Function and Structural Theory of Thermoeconomics, *Energies*, *138* (2020) pp. 1-21

[19] Valero, A., *et al*., On the Thermoeconomic Approach to the Diagnosis of Energy System Malfunctions. Part 1: The TADEUS Problem and Part 2: Malfunction Definitions and Assessment, *Energy*, 29 (2004), pp.1875-1907

[20] Maziyar, H., *et al*., Thermoeconomic Analysis and Optimization of a Geothermal-Driven Multi-Generation System Producing Power, Freshwater, and Hydrogen, *Energy*, *247* (2022), pp. 123434

Submitted: 17.04.2024.
Revised: 17.06.2024.
Accepted: 30.07.2024.